Pergamon

Int. J. Heat Mass Transfer. Vol. 37, No. 5, pp. 865–875, 1994
Elsevier Science Ltd
Printed in Great Britain.
0017-9310/94 \$6.00+0.00

An approximate equation for the vapour-side heat-transfer coefficient for condensation on low-finned tubes

J. W. ROSE

Queen Mary and Westfield College, University of London, London, U.K.

(*Received* 2 *March* 1993)

Abstract—Simplifying approximations, together with dimensional analysis, have been used to obtain a formula for the relation between the heat flux and vapour-side temperature difference for condensation on low, integral-finned tubes. The final result involves two unknown (disposable) constants which have been determined from heat-transfer data. The resulting equation is found to be in satisfactory agreement with experimental data from 11 investigations with various condensing fluids and a range of fin and tube geometries.

INTRODUCTION

SURFACE tension, in the presence of changing curvature of the interface between vapour and condensate, gives rise to a pressure gradient which influences the motion of the condensate film. For a horizontal smooth tube, changes in interface curvature are, except near the bottom of the tube, small and the effect of surface tension is weak, as is evidenced by the success of the Nusselt [1] theory. For a finned tube, however, abrupt changes in curvature of the condensate surface occur near the tips and roots of the fins. At the same time the presence of fins on a horizontal tube leads to capillary retention of liquid between fins on the lower part of the tube. Thus the presence of fins on a condenser tube affects the heat transfer in three ways: (1) as in single phase heat transfer, the fins provide additional heat-transfer surface, (2) the surface tension-induced pressure gradient in the condensate film assists drainage from parts of the surface, and thereby enhances the heat transfer by reducing the film thickness, and (3) capillary retention of condensate adversely affects the heat transfer.

ENHANCEMENT RATIO

It is convenient to compare the performance of finned and smooth tubes in terms of an 'enhancement ratio', i.e. heat-transfer coefficient for the finned tube divided by heat-transfer coefficient for smooth tube, both based on the smooth-tube area. Thus, in design calculations, one would treat a finned tube as a smooth tube with vapour-side, heat-transfer coefficient equal to the smooth-tube (e.g. Nusselt) value multiplied by the enhancement ratio. However, as discussed in Masuda and Rose [2, 3], it is important to define enhancement ratio carefully. In condensation, the heat flux does not vary linearly with vapour-to-surface temperature difference, i.e. the heat-transfer coefficient is not independent of heat flux or temperature difference. Moreover, there is no reason to presume that the heat flux-temperature difference relation will be similar for a finned and smooth tube. An enhancement ratio can only strictly be defined at a particular temperature difference or heat flux (same for both smooth and finned tube). However, experiment has shown that for condensation on low-finned tubes, the heat flux-temperature difference dependence is generally not far from $q \propto \Delta T^{3/4}$ as given by the Nusselt theory for a smooth tube. If this were strictly true for both finned and smooth tube, the enhancement ratio would be independent of ΔT or q. This is particularly convenient since we can then ascribe an enhancement ratio to a given tube (and condensing fluid) without specifying ΔT or q. As pointed out by Masuda and Rose [2, 3], it is important to note that the enhancement ratio at the same ΔT, is not the same as the enhancement ratio at the same q.

Defining enhancement ratio at the same ΔT by

$$\varepsilon_{\Delta T} = \frac{\alpha_{\text{finned tube}}}{\alpha_{\text{smooth tube}}} = \frac{(q/\Delta T)_{\text{finned tube}}}{(q/\Delta T)_{\text{smooth tube}}} = \frac{q_{\text{finned tube}}}{q_{\text{smooth tube}}} \tag{1}$$

and enhancement ratio at the same q by

$$\varepsilon_{q} = \frac{\alpha_{\text{finned tube}}}{\alpha_{\text{smooth tube}}} = \frac{(q/\Delta T)_{\text{finned tube}}}{(q/\Delta T)_{\text{smooth tube}}} = \frac{\Delta T_{\text{smooth tube}}}{\Delta T_{\text{finned tube}}} \tag{2}$$

where the heat flux and heat-transfer coefficient are based, in both bases, on the smooth tube surface area. $\varepsilon_{\Delta T}$ and ε_q will depend in general on ΔT and q, respectively. However, if $q \propto \Delta T^{3/4}$ for both smooth and finned tubes, it is evident that $\varepsilon_{\Delta T}$ and ε_q are independent of ΔT and q and that

$$\varepsilon_q = (\varepsilon_{\Delta T})^{4/3}. \tag{3}$$

NOMENCLATURE

A	constant in equation (29)
B	constant in equation (29)
B_f	value of B for fin flank
B_1	constant in equation (47)
B_s	value of B for interfin tube surface
B_t	value of B for fin tip
b	spacing between fin flanks at fin tip
C	constant in equation (19)
d	tube diameter
d_o	diameter at fin tip
d_r	diameter at fin root
f	defined in equation (16)
f_f	fraction of unflooded part of fin flank blanked by retained condensate at fin root
f_s	fraction of unflooded part of interfin tube surface blanked by retained condensate at fin root
G_f	defined in equation (44)
G_s	defined in equation (46)
G_t	defined in equation (42)
g	specific force of gravity
h	radial height of fin
h^*	local vertical fin height
h_v	effective mean vertical fin height
h_{fg}	specific enthalpy of evaporation
J	$\sigma/\rho g r^2$
K	$\mu k \Delta T/r^3 \rho\tilde{\rho} g h_{fg}$
k	thermal conductivity of condensate
L	height of vertical plane surface
n	constant in equation (19)
P	pressure
Q_f	total heat-transfer rate over one pitch length for a finned tube
Q_s	total heat-transfer rate to smooth tube over a length equal to one pitch length of finned tube
q	heat flux
q_f	heat flux for fin flanks
q_s	heat flux for tube surface between fins
q_{smooth}	heat flux for smooth tube
q_t	heat flux for fin tip
r	radius of smooth tube
r_c	radius of curvature of condensate surface
r_r	radius at fin root
$\tilde{r}$	$r+\delta$
s	spacing between fin flanks at fin root
T_f	defined in equation (43)
T_s	defined in equation (45)
T_t	defined in equation (41)
t	fin thickness at fin tip
V	condensation volume flux
x, x_1, x_2	linear dimension, distance along surface
x_g	appropriate linear dimension for condensate flow governed by gravity
x_σ	appropriate linear dimension for condensate flow governed by surface tension.

Greek symbols

α	heat-transfer coefficient based on smooth tube area at fin root diameter
β	half-angle at fin tip, i.e. angle between fin flank and plane normal to tube axis
Δ	δ/r
ΔT	vapour-to-surface temperature difference
δ	condensate film thickness
$\varepsilon_{\Delta T}$	enhancement ratio (heat-transfer coefficient for finned tube divided by heat-transfer coefficient for smooth tube, both based on smooth tube area at fin root diameter and for same ΔT)
ε_q	enhancement ratio (heat-transfer coefficient for finned tube divided by heat-transfer coefficient for smooth tube, both based on smooth tube area at fin root diameter and for same q)
θ	angle measured from top of tube
μ	viscosity of condensate
$\xi(\theta)$	function defined in equation (25) and given approximately in equation (26)
ρ	density of condensate
ρ_v	density of vapour
$\tilde{\rho}$	$\rho-\rho_v$
σ	surface tension
ϕ	condensate retention or 'flooding' angle measured from top of tube.

Thus, for a value of $\varepsilon_{\Delta T}$ of 7, such as may be found with refrigerants, ε_q is in excess of 13.

In the presence of appreciable vapour velocity, the enhancement ratio is a less useful quantity since q is not proportional to a power of ΔT and vapour velocity affects the heat-transfer coefficient for a smooth tube more strongly than for a finned tube. Thus the enhancement ratio, for a given vapour velocity (same for finned and smooth tube), would decrease with increasing vapour velocity. However, upper and lower bounds for the heat-transfer coefficient for a finned tube in the presence of significant vapour velocity are given by multiplying the quiescent-vapour enhancement ratio by the forced- and free-convection, smooth-tube coefficients, respectively.

BEATTY–KATZ [4] MODEL

This early model ignores surface tension effects and treats both the fin flanks and the cylindrical interfin tube surface using the Nusselt approach with condensate flow on the vertical plane, and horizontal cylindrical, surfaces controlled by gravity and viscosity. The Beatty and Katz model can give acceptable results for low surface tension fluids. This is partly because surface tension effects are small and partly because the condensate retention and drainage enhancing effects of surface tension cancel each other to some extent.

Beatty and Katz [4] gave their result for a finned tube in the form of a Nusselt expression for a smooth tube with an 'equivalent diameter'. The Beatty and Katz approach can be used instead to obtain an expression for the enhancement ratio. Thus for a tube with rectangular section fins ($b = s$) the enhancement ratio $\varepsilon_{\Delta T}$ (ratio of the heat-transfer coefficients for the finned and smooth tubes, both based on the smooth tube area at fin root diameter, d_r, and for the same ΔT) is given by

$$\varepsilon_{\Delta T} = \frac{q_f(d_o^2 - d_r^2)/2 + q_t d_o t + q_s d_r s}{q_{\text{smooth}} d_r (b+t)} \tag{4}$$

where q_f, q_s and q_t are the mean heat fluxes for the fin flanks, interfin tube surface and fin tip, respectively. Taking $q_s = q_{\text{smooth}}$ and treating these surfaces on the basis of the Nusselt theory with negligible temperature drop in the fins for high conductivity, low-fin tubes, one obtains

$$\varepsilon_{\Delta T} = \frac{\dfrac{0.943}{0.728}\left(\dfrac{d_r}{h_v}\right)^{1/4}\left(\dfrac{d_o^2 - d_r^2}{2d_r}\right) + t\left(\dfrac{d_o}{d_r}\right)^{3/4} + s}{b+t} \tag{5}$$

where h_v is the mean effective plate height for the fin flanks.

For low fins, when $d_o \approx d_r \approx d$, equation (5) becomes

$$\varepsilon_{\Delta T} = 1 + \frac{0.943}{0.728}\left(\frac{2h}{b+t}\right)\left(\frac{d}{h_v}\right)^{1/4}. \tag{6}$$

The 'proper mean value' of the vertical fin height h_v used by Beatty and Katz approximates, for low fins, to

$$h_v = \pi h. \tag{7a}$$

For low fins ($h \ll d_r$), this approximates to twice the average value of the *vertical* height from fin root to fin tip. If condensate drains from the fin flanks to the interfin tube surface and thence to the lowest part of the tube before draining along the flanks and leaving the tube, a more appropriate mean vertical fin height would be half the Beatty and Katz value, i.e.

$$h_v = \pi h/2. \tag{7b}$$

Since h_v occurs to the power 1/4 in equations (5) and (6), the value of $\varepsilon_{\Delta T}$ is less than 20% higher when using h_v from equation (7b) rather than from equation (7a).

Note that equations (5) and (6) contain only geometric variables so that, according to the Beatty and Katz model, the enhancement ratio, for a given fin and tube geometry, is the same for all fluids.

CONDENSATE RETENTION

Equation (6) shows that the Beatty–Katz model predicts that $\varepsilon_{\Delta T}$ increases continuously as the interfin space decreases. In practice, there exists an optimum (for fixed values of the other dimensions and for a given fluid) below which $\varepsilon_{\Delta T}$ decreases due to increasing condensate retention (neglected in the Beatty–Katz model).

For trapezoidal-section low fins, with fin height greater than half the distance between adjacent fin tips ($h > b/2$) an equation for calculating the retention angle ϕ, i.e. the angle measured from the top of the tube to the position at which the whole of the interfin space is filled with retained liquid, has been obtained by Honda *et al.* [5]:

$$\phi = \cos^{-1}\{(4\sigma\cos\beta/\rho g b d_o) - 1\}. \tag{8}$$

(Note that when $\sigma\cos\beta/\rho g b d_o > 0.5$ the interfin space is fully flooded and ϕ should be set to zero.) Virtually the same result was obtained independently by Rudy and Webb [6, 7]. Equation (8) has been well verified experimentally by several investigators.

Equation (8) was also obtained as a special case, in a more general treatment by Masuda and Rose [8], who demonstrated, in addition, that liquid is also retained in the form of 'wedges' at the fin roots on the upper part of a tube previously regarded as unflooded (see Fig. 1).

As shown by Masuda and Rose [8] and illustrated in Fig. 1, parts of the unflooded fin flank and interfin tube space are effectively insulated by retained condensate. Masuda and Rose [8] showed that, for parallel-side fins with sharp-edged fin roots, the fractions f_f and f_s, of the unflooded parts of the flank and interfin tube space which are blanked can be approximated by

$$f_f = \frac{2\sigma}{\rho g d_r h}\frac{\tan(\phi/2)}{\phi} \tag{9}$$

and

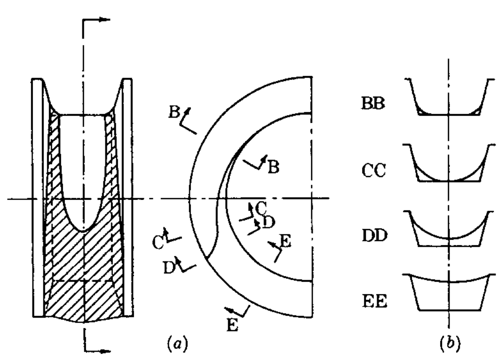

FIG. 1. Configuration of retained liquid. Reproduced from Masuda and Rose [8].

$$f_s = \frac{4\sigma}{\rho g d_r s}\cdot\frac{\tan(\phi/2)}{\phi}. \tag{10}$$

For trapezoidal fins with sharp-edged fin roots, it is readily shown that f_f and f_s become:

$$f_f = \frac{1-\tan(\beta/2)}{1+\tan(\beta/2)}\cdot\frac{2\sigma\cos\beta}{\rho g d_r h}\cdot\frac{\tan(\phi/2)}{\phi} \tag{11}$$

$$f_s = \frac{1-\tan(\beta/2)}{1+\tan(\beta/2)}\cdot\frac{4\sigma}{\rho g d_r s}\cdot\frac{\tan(\phi/2)}{\phi}. \tag{12}$$

Note that owing to approximations in the derivations of f_f and f_s, the quantities given by equations (9)–(12) can, in some circumstances, marginally exceed unity. In these cases the relevant quantity should be set to unity. Note also that for fins with appropriately radiused† fin roots (see Masuda and Rose [8]), f_f and f_s would be zero and estimates needed of the appropriate values to assign to h and s.

SURFACE TENSION-INDUCED PRESSURE GRADIENT

More complicated than condensate retention is the effect of surface tension on the motion of the condensate film highlighted by Gregorig [9] in relation to condensation on a fluted surface. Change in surface curvature along a condensate film results in corresponding changes in the pressure drop across the vapour–liquid interface. This, in turn, gives rise to a pressure gradient in the film. In the presence of sharp changes in surface curvature, such as occur in a condensate film near the tips and roots of fins, large pressure gradients are set up which have a significant effect on the condensate motion and hence on the film thickness. For condensation on finned tubes this is an important aspect of the mechanism of heat-transfer enhancement.

Even for the relatively straightforward two-dimensional case of the horizontal tube shown in Fig. 2, where the velocity vectors for the condensate flow and gravity are in the same plane, considerable complexity arises when the surface tension pressure gradient is included. The pressure gradient in the film in the direction along the surface is given by

$$\frac{dP}{dx} = \sigma\frac{d}{dx}\left(\frac{1}{r_c}\right) \tag{13}$$

where r_c is the radius of curvature of the surface of the condensate film, given by

$$r_c = \frac{\{\tilde{r}^2+(d\tilde{r}/d\theta)^2\}^{3/2}}{\tilde{r}^2+2(d\tilde{r}/d\theta)^2-\tilde{r}\,d^2\tilde{r}/d\theta^2} \tag{14}$$

where $\tilde{r} = r+\delta$.

Using the same approximations as in the Nusselt

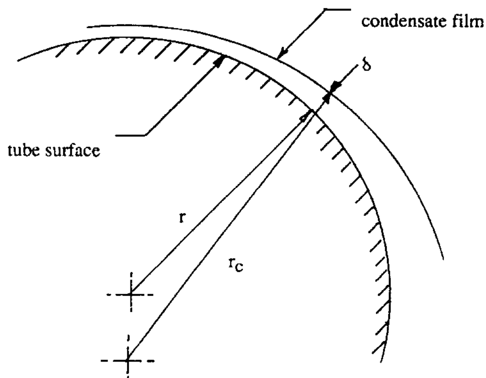

FIG. 2. Condensate film on a horizontal tube.

theory, but including the pressure gradient term in the momentum balance, the following fourth-order equation for the local condensate film thickness is obtained.

$$\frac{d}{d\theta}\left\{\Delta^3\sin\theta - J\Delta^3\frac{df}{d\theta}\right\} = \frac{3K}{\Delta} \tag{15}$$

where

$$\Delta = \delta/r$$
$$J = \sigma/\rho g r^2$$
$$K = \mu k\Delta T/r^3\rho\tilde{\rho} g h_{fg}$$

and

$$f = \frac{(1+\Delta)^2+2(d\Delta/d\theta)^2-(1+\Delta)\,d^2\Delta/d\theta^2}{\{(1+\Delta)^2+(d\Delta/d\theta)^2\}^{3/2}}. \tag{16}$$

It may be seen that, when gravity dominates over surface tension, i.e. $J \to 0$, the Nusselt first-order equation for the film thickness is recovered.

HEAT-TRANSFER MODELS INCLUDING SURFACE TENSION

All treatments of this problem to date have been based on a two-dimensional approach. Either gravity has been neglected when considering the surface tension driven radially inward flow of condensate on the fin flank, or only the radial component of gravity has been included. In some cases (e.g. Karkhu and Borovkov [10], Rifert [11], Webb *et al.* [12], Adamek and Webb [13]) the problem has been greatly simplified by assuming a uniform pressure gradient along the fin flank, with further assumptions about the curvature of (and hence pressure in) the film at the fin tip and fin root. A more accurate treatment by Honda and Nozu [14] (who solved equation (15) numerically, using the radial component of gravity and with assumptions about the film curvature at the fin tip and root to specify a sufficient number of boundary conditions), indicated that the pressure gradient on the fin flank was far from uniform. As expected on physical grounds, a sharp pressure peak occurs near

† i.e. an arc touching both fin flanks and the interfin-tube space at the fin root diameter when

$r_r = ((b/2)-h\tan\beta)(1+\tan(\beta/2))/(1-\tan(\beta/2))$.

the fin tip due to the convex curvature of the condensate film, and a pressure minimum occurs at the fin root where the film surface is concave. Along much of the fin flank, changes in curvature and hence in pressure, are smaller.

The present author has long held the view that there exists a need for an approximate model, in the form of an algebraic expression similar to that of Beatty and Katz [4], but including surface tension effects. Such an approach is given below.

DIMENSIONAL ANALYSIS

Following the procedure which has been used successfully in single-phase convective heat transfer problems, dimensional analysis may be used to establish the relevant dimensionless parameters and a simple form assumed for the relationship between them. For the Nusselt problem, where the condensate flow is influenced only by gravity and viscosity, and where the surface geometry is characterized by a single linear dimension (e.g. diameter of horizontal tube or height of vertical plate) we have

$$\delta = f(V, \tilde{\rho}g, \mu, x) \tag{17}$$

where

δ = mean condensate film thickness, i.e. for pure conduction in the film $q = k\Delta T/\delta$, where q is the mean heat flux for the surface,
V = mean volume condensation flux per area of surface,
$\tilde{\rho}g$ = net downward force per volume,
μ = viscosity of condensate,
x = linear dimension.

Dimensional analysis then gives

$$\frac{\delta}{x} = \phi\left(\frac{\mu V}{\tilde{\rho}gx^2}\right). \tag{18}$$

As in many convective heat-transfer problems we take, for the form of the function in equation (18)

$$\frac{\delta}{x} = C\left(\frac{\mu V}{\tilde{\rho}gx^2}\right)^n \tag{19}$$

where C and n are constants.

Noting that

$$V = \frac{q}{h_{fg}\rho} \tag{20}$$

and

$$q = \frac{k\Delta T}{\delta} \tag{21}$$

equation (19) may be compared with Nusselt theory which gives

$$\frac{\delta}{d} = \frac{1}{0.728^{4/3}}\left(\frac{\mu V}{\tilde{\rho}gd^2}\right)^{1/3} \tag{22}$$

for the horizontal tube, and

$$\frac{\delta}{L} = \frac{1}{0.943^{4/3}}\left(\frac{\mu V}{\tilde{\rho}gL^2}\right)^{1/3} \tag{23}$$

for the vertical plate.

Anticipating that, when treating the interfin tube surface for a finned tube, we shall need the mean condensate film thickness for that part of a horizontal tube between the top and the angle θ from the vertical (this arises because condensate retention obscures the lower part of the interfin space) we note that the Nusselt theory gives

$$\frac{\delta}{d} = \frac{1}{\xi(\theta)}\left(\frac{\mu V}{\tilde{\rho}gd^2}\right)^{1/3} \tag{24}$$

where

$$\xi(\theta) = \frac{1}{2^{1/3}\theta^{4/3}}\left[\int_0^\theta \left\{\frac{\int_0^\theta (\sin\theta)^{1/3}\,d\theta}{(\sin\theta)^{4/3}}\right\}^{-1/4} d\theta\right]^{4/3}. \tag{25}$$

$\xi(\theta)$ is given, approximately, by

$$\xi(\theta) = 0.874 + 0.1991\times10^{-2}\theta - 0.2642\times10^{-1}\theta^2 + 0.5530\times10^{-2}\theta^3 - 0.1363\times10^{-2}\theta^4. \tag{26}$$

Equation (26), obtained by fitting numerically-obtained values from equation (25), is accurate to within 0.15% except near $\theta = \pi$ where the maximum error is 0.5%.

The fact that dimensional analysis and the assumed form of equation (19) gives the correct result for the Nusselt problem (apart from the numerical values of two constants) gives us confidence in applying the same method when surface tension is important. If we replace the gravity term in equation (17) by the surface tension, σ, we obtain from dimensional analysis

$$\frac{\delta}{x} = \psi\left(\frac{\mu V}{\sigma}\right). \tag{27}$$

For condensation on a surface such as a fin tip, fin flank, or the surface of tube between fins, both surface tension and gravity are important and the characteristic length is different for each. For this case dimensional analysis suggests

$$\frac{\delta}{x_1} = \zeta\left(\frac{\mu V}{\tilde{\rho}gx_2^2}, \frac{\mu V}{\sigma}\right) \tag{28}$$

where x_1 and x_2 are appropriate characteristic dimensions.

We provisionally propose, for equation (28), the simple form

$$\delta = \left(\frac{\mu V}{\dfrac{A\tilde{\rho}g}{x_g} + \dfrac{B\sigma}{x_\sigma^3}} \right)^{1/3} \tag{29}$$

where A and B are constants and x_g and x_σ are appropriate characteristic lengths for gravity and surface tension driven flows, respectively. When σ is set to zero, equation (29) reduces, with the appropriate values of A and x_g, to equation (22), (23) or (24). When g is set to zero, equation (29) gives, for equation (27)

$$\frac{\delta}{x_\sigma} = \frac{1}{B^{1/3}} \left(\frac{\mu V}{\sigma} \right)^{1/3}. \tag{30}$$

Since $\delta \propto V^{1/3}$, as in the Nusselt theory, equation (29) leads to an expression for the 'enhancement ratio' which is independent of ΔT, as has been found experimentally to be approximately true.

It is interesting to note that, for a given condensation rate, the film thickness depends on the first power of the linear dimension for surface tension-driven condensate flow (see equation (30)), while for gravity-driven flow the film thickness varies as the linear dimension raised only to the power 1/3 (see equations (22) and (23)). We therefore anticipate that, with decreasing dimensions (fin height, fin thickness, interfin tube space) the effect of surface tension on heat-transfer will increasingly dominate over that of gravity. This is illustrated by equation (29).

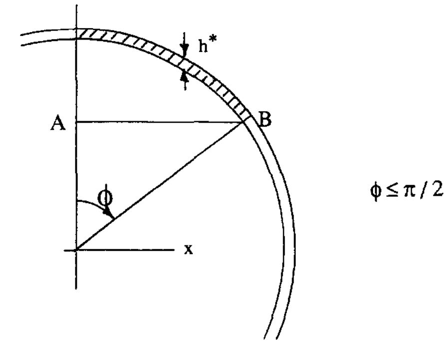

$$h_v = \frac{1}{AB} \int_0^{AB} h^* \, dx = \text{shaded area} / AB \approx h\phi / \sin\phi$$

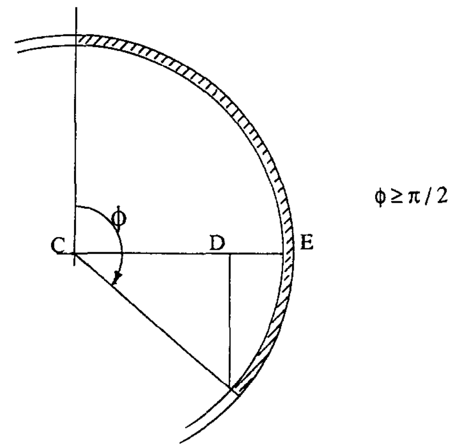

$$h_v = \text{shaded area} / (CE + DE) \approx h\phi / (2 - \sin\phi)$$

FIG. 3. Approximation for mean vertical height of fin.

ENHANCEMENT RATIO FOR FINNED TUBE

When applying equation (29) to the fin tip, where there is no retained condensate, $A = 0.728^4$, $x_g = d_o$, $x_\sigma = t$ and B is an unknown constant B_t. For the unflooded part of the fin flanks, we take $A = 0.943^4$, $x_g = h_v$, the mean vertical fin height. As indicated in Fig. 3, for low fins, h_v may be approximated by

$$h_v = h\phi/\sin\phi \quad \text{for } \phi \leqslant \pi/2 \tag{31}$$

$$h_v = h\phi/(2-\sin\phi) \quad \text{for } \phi \geqslant \pi/2. \tag{32}$$

For the fin flanks $x_\sigma = h$ and B is an unknown constant B_f. For the unflooded part of the tube space between fins $A = (\xi(\phi))^3$, $x_g = d_r$, $x_\sigma = s$ and B is an unknown constant B_s. Different constants, B, are used for the fin tip, flank and interfin tube space because the boundary conditions for surface tension drainage are different for three surfaces (see Fig. 4) and the direction of the surface tension pressure gradient in relation to that of gravity is not the same in all three cases.

Using equations (20) and (21), with the values of A, B, x_g and x_σ given above and neglecting temperature drop in the fins, equation (29) can be rearranged to give the mean surface heat flux for the fin tip, fin flanks and interfin space.

For the fin tip:

$$q_t = \left\{ \frac{\rho h_{fg} k^3 \Delta T^3}{\mu} \left(\frac{0.728^4 \tilde{\rho} g}{d_o} + \frac{B_t \sigma}{t^3} \right) \right\}^{1/4}. \tag{33}$$

For the fin flanks:

$$q_f = \left\{ \frac{\rho h_{fg} k^3 \Delta T^3}{\mu} \left(\frac{0.943^4 \tilde{\rho} g}{h_v} + \frac{B_f \sigma}{h^3} \right) \right\}^{1/4}. \tag{34}$$

For the interfin tube space:

$$q_s = \left\{ \frac{\rho h_{fg} k^3 \Delta T^3}{\mu} \left(\frac{(\xi(\phi))^3 \tilde{\rho} g}{d_r} + \frac{B_s \sigma}{s^3} \right) \right\}^{1/4}. \tag{35}$$

Assuming no heat transfer to the 'flooded' and blanked parts of the fin flanks and interfin tube space, the heat-transfer rate to a tube length of one fin pitch (fin tip, two fin flanks, interfin tube surface) is given, for *rectangular section fins* ($s = b$, $\beta = 0$), by

$$Q_f = \pi d_o t q_t + \frac{\phi}{\pi} \left\{ \frac{(1-f_f)\pi(d_o^2 - d_r^2)}{2} q_f + (1-f_s)\pi d_r s q_s \right\}. \tag{36}$$

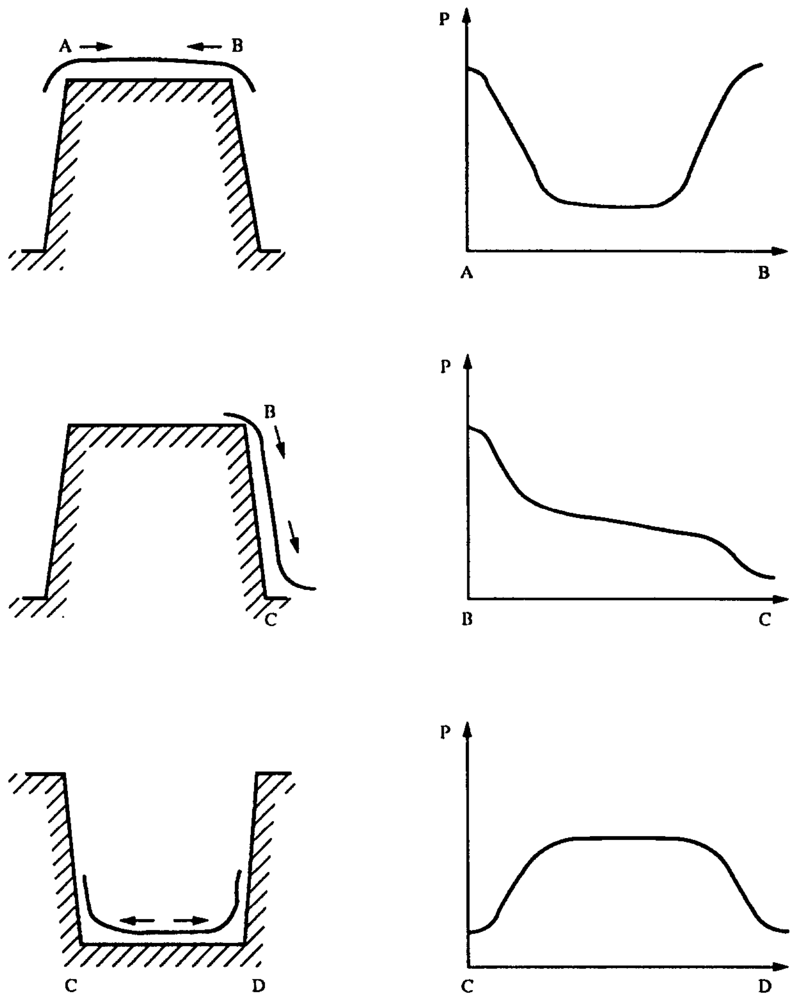

FIG. 4. Sketch of surface tension induced flow and pressure distributions on fin surfaces.

The heat-transfer rate to the same length of a smooth tube with diameter equal to the fin root diameter is

$$Q_s = \pi d_r (b+t) q_{\text{smooth}}. \tag{37}$$

The Nusselt theory gives

$$q_{\text{smooth}} = 0.728\left(\frac{\rho h_{fg} k^3 \Delta T^3}{\mu}\frac{\tilde{\rho} g}{d_r}\right)^{1/4}. \tag{38}$$

Then, using equations (33)–(38) the enhancement ratio for the same ΔT,

$$\varepsilon_{\Delta T} = \frac{Q_f/\Delta T}{Q_s/\Delta T} = \frac{Q_f}{Q_s} \tag{39}$$

may be written

$$\varepsilon_{\Delta T} = \frac{d_o}{d_r}\frac{t}{(b+t)}T_t + \frac{\phi}{\pi}(1-f_f)\left(\frac{d_o^2-d_r^2}{2d_r(b+t)}\right)T_f + \frac{\phi}{\pi}(1-f_s)\frac{s}{(b+t)}T_s \tag{40}$$

where

$$T_t = \left\{\frac{d_r}{d_o} + \frac{B_t G_t}{0.728^4}\right\}^{1/4} \tag{41}$$

$$G_t = \frac{\sigma d_r}{\tilde{\rho} g t^3} \tag{42}$$

$$T_f = \left\{\left(\frac{0.943}{0.728}\right)^4 \frac{d_r}{h_v} + \frac{B_f G_f}{0.728^4}\right\}^{1/4} \tag{43}$$

$$G_f = \frac{\sigma d_r}{\tilde{\rho} g h^3} \tag{44}$$

$$T_s = \left\{\frac{(\xi(\phi))^3}{0.728^4} + \frac{B_s G_s}{0.728^4}\right\}^{1/4} \tag{45}$$

$$G_s = \frac{\sigma d_r}{\tilde{\rho} g s^3}. \tag{46}$$

The following points may be noted.

1. The enhancement ratio given by equation (40) is independent of ΔT.
2. The only thermophysical property in equation (40) is the ratio $\sigma/\tilde{\rho}$.
3. The three unknowns B_t, B_f and B_s remain to be found empirically.
4. Since conduction resistance in the fin has been neglected, the validity of equation (40) may be expected to decrease with decreasing thermal conductivity of the tube material and with increasing 'slenderness ratio' (h/t) of the fins.
5. Equation (40) gives the heat-transfer coefficient for a finned tube (based on the smooth tube area with fin root diameter) divided by that for a smooth tube with diameter equal to that at the fin root, for the same ΔT.
6. When $\sigma \cos\beta/\rho g b d_o > 0.5$, i.e. the argument in equation (8) exceeds unity, the interfin space is 'fully flooded' and ϕ should be set to zero.

Table 1. Key to data in Figs. 5 and 6

Symbol	Reference	Fluid
	Figs. 5 and 6	
□	Briggs *et al.* [17]	steam
×	Briggs *et al.* [17]	R113
✿	Briggs *et al.* [17]	glycol
◇	Wen [18]	steam
▽	Wen [18]	R113
△	Wen [18]	glycol
#	Wanniarachchi *et al.* [19]	steam
+	Wanniarachchi *et al.* [20]	steam
◆	Marto *et al.* [21]	R113
⊞	Michael *et al.* [22]	R113
○	Honda *et al.* [5]	R113
●	Honda *et al.* [5]	methanol
	Fig. 6	
■	Honda *et al.* [5]	R113
▲	Honda *et al.* [5]	methanol
✚	Carnavos *et al.* [23]	R11
◆	Webb *et al.* [12]	R11
*	Katz *et al.* [24]	R12
<	Beatty and Katz [4]	various

DETERMINATION OF THE CONSTANTS

It is difficult to decide which data should be included in the determination of the constants. Different investigators have used different methods to determine the vapour-side coefficient (direct measurement of wall temperature or from overall temperature difference using pre-determined coolant-side correlation or some form of 'Wilson Plot'). In some cases significant vapour velocity may have been present. Moreover, $\varepsilon_{\Delta T}$ is not strictly independent of ΔT.

When determining the unknown constants by minimization of the sum of squares of residuals (measured minus calculated values) of $\varepsilon_{\Delta T}$, appropriate weighting factors should be employed according to the accuracy or reliability of the various data sets. At this point no attempt has been made to obtain definitive values of the constants. Minimization procedures have been carried out using data for copper tubes with rectangular section fins (with sharp-edged fin roots) which were both readily available and considered to be of high accuracy. These data were obtained from seven investigations (identified in Table 1) in which four different condensing fluids were used with 41 different tube/fin geometries. No weighting factors were used.

Curve fits were also done with the constants B_t, B_f, and B_s set equal and when allowed to take different values. The constants were determined by minimizing the sum of squares of relative residuals of $\varepsilon_{\Delta T}$ (one minus ratio of measured to calculated value). The standard deviations were never more than 23%. The approximate nature of equation (40) and the fact that the constants B_t, B_f, and B_s did not generally differ greatly when found separately, led to the decision to set these constants equal. Partially to account for the fact that condensate drainage from the fin flanks would affect both gravity and surface tension contributions to the heat transfer at the interfin tube space a 'lead' constant B_l was introduced in the last term of equation (40), thus

$$\varepsilon_{\Delta T} = \frac{d_o}{d_r}\frac{t}{(b+t)}T_t + \frac{\phi}{\pi}\frac{(1-f_f)}{\cos\beta}\left(\frac{d_o^2-d_r^2}{2d_r(b+t)}\right)T_f + \frac{\phi}{\pi}(1-f_s)B_l\frac{s}{(b+t)}T_s. \quad (47)$$

(Note that $\cos\beta$ has been inserted in the denominator of the second term in equation (47) to extend the applicability to *trapezoidal* section fins.)

Although on physical grounds there is no reason to expect the tip, flank and interfin space constants to have the same value, and the lead constant, B_l might have been expected to be less than unity, an excellent fit was obtained with $B_t = B_f = B_s = 0.143$ and $B_l = 2.96$. The standard deviation was 12.4%.

COMPARISON WITH EXPERIMENTAL DATA

Figure 5 compares measured and calculated (equation (47) with the above constants) values of $\varepsilon_{\Delta T}$ for the data used to determine the constants. It may be seen that virtually all of the data are represented to better than 20% by equation (47) with the constants given above. In Fig. 6 data from investigations not used in obtaining the constants have also been included. In the case of the data of Webb *et al.* [12], where significant fin root curvature was present, f_f and f_s have been set to zero. The relatively recent data of Sukhatme *et al.* [15] have been omitted since the fins were very thin ($0.06 \leqslant t$ (mm) $\leqslant 0.13$) and consequently the thickness was subject to significant uncertainty, while, for most of the data, the tubes were fully flooded when only the fin tips contribute to the heat transfer. Under these conditions the predictions are susceptible to large uncertainty. It is evident that equa-

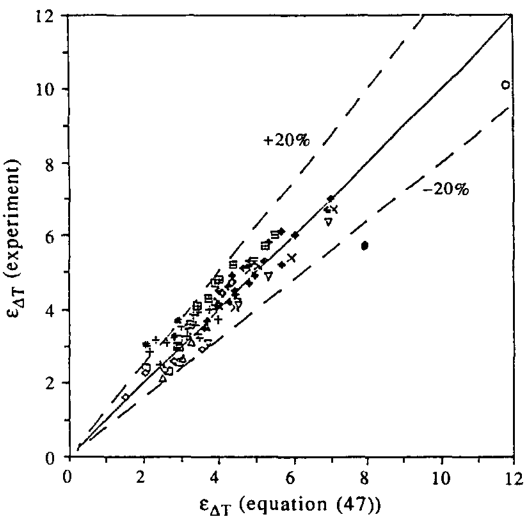

Fig. 5. Comparison of equation (47) with data used to determine constants. (Symbols defined in Table 1.)

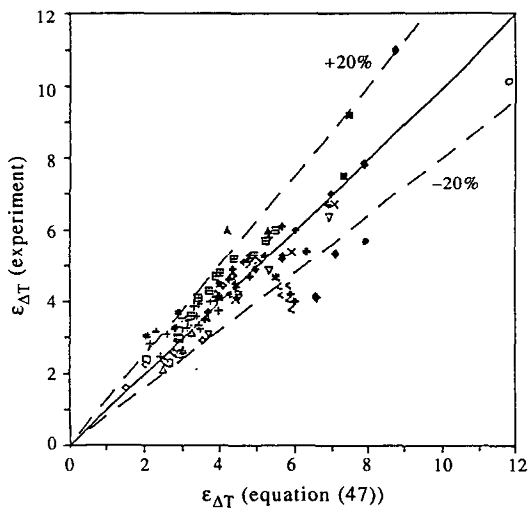

Fig. 6. Comparison of equation (47) with all data. (Symbols defined in Table 1.)

tion (47) is in good agreement with most of the available data.

Figure 7 shows a comparison between experiment and equation (47) for the dependence of $\varepsilon_{\Delta T}$ on fin spacing (other dimensions fixed) for copper tubes and three condensing fluids. The general agreement, and particularly the prediction of the optimum fin spacing, is satisfactory. The slope discontinuity at low fin spacing occurs when $\phi = 0$, i.e. when the whole of the interfin space is flooded and only the fin tip contributes to the heat transfer. For smaller fin spacings only the first term in equation (47) is used and $\varepsilon_{\Delta T}$ increases with increasing fin tip area.

Figure 8 compares calculated and experimental values of $\varepsilon_{\Delta T}$ for three fluids and for copper tubes with various fin heights but otherwise identical fin and tube geometry. As in Fig. 7, agreement between experiment and equation (47) is generally satisfactory. The slope discontinuity at small fin heights occurs when the fin height is such that $f_f = 1$. For lower fin heights there is no heat-transfer contribution from the fin flanks.

Figure 9 shows excellent agreement between equation (47) and experimental data giving the dependence of $\varepsilon_{\Delta T}$ on fin spacing for a larger diameter tube and for two fluids.

Figure 10 compares calculated and experimental values of $\varepsilon_{\Delta T}$ for copper tubes with different fin thickness but otherwise the same geometry. The agreement is good for R113 but for steam the calculated values are around 25% lower than the measurements. For this fluid and geometry (fin spacing, fin height, tube diameter) agreement with theory was least satisfactory of all the data used in determining the constants.

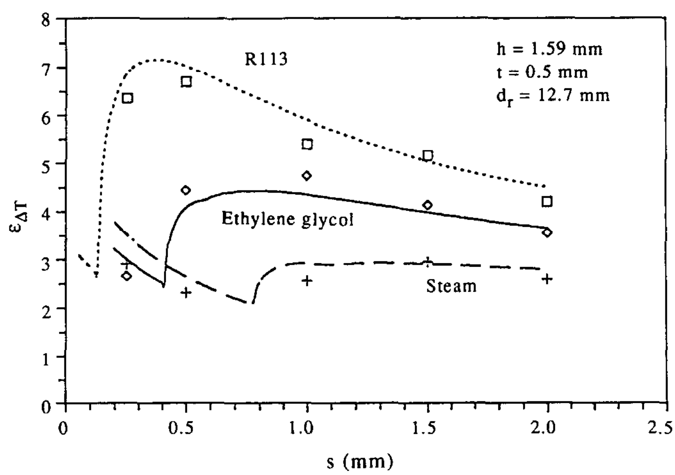

Fig. 7. Dependence of $\varepsilon_{\Delta T}$ on fin spacing. Comparison of equation (47) with data of Wen [18] and Briggs *et al.* [17].

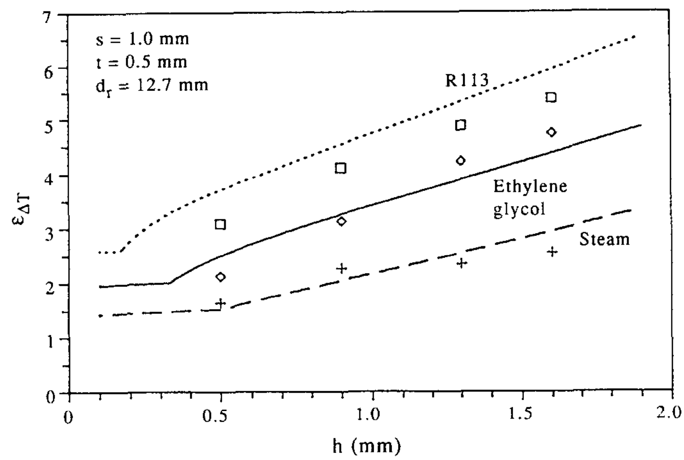

Fig. 8. Dependence of $\varepsilon_{\Delta T}$ on fin height. Comparison of equation (47) with data of Wen [18].

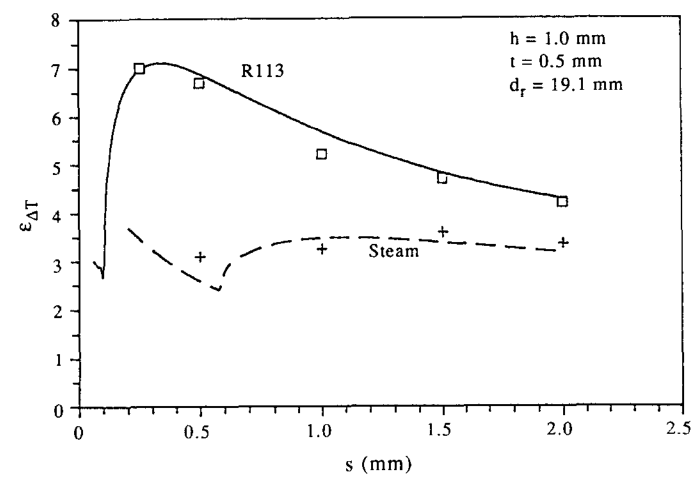

Fig. 9. Dependence of $\varepsilon_{\Delta T}$ on fin spacing. Comparison of equation (47) with data of Wanniarachchi *et al.* [19, 20] and Marto *et al.* [21].

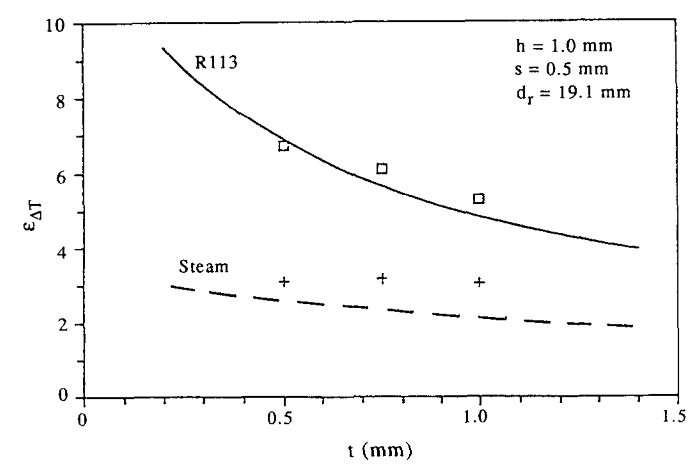

Fig. 10. Dependence of $\varepsilon_{\Delta T}$ on fin thickness. Comparison of equation (47) with data of Wanniarachchi *et al.* [19, 20] and Marto *et al.* [21].

CONCLUDING REMARKS

1. Equation (47) agrees satisfactorily with most of the available experimental data for condensation of various fluids on low-finned copper tubes.

2. In design calculations, a low-finned tube should be treated as a smooth tube with the fin root diameter and a vapour-side, heat-transfer coefficient equal to the plain tube value (e.g. Nusselt) multiplied by $\varepsilon_{\Delta T}$ as given by equation (47). To obtain the heat-transfer coefficient based on the smooth tube area with diameter d_o, the appropriate ratio by which to multiply the heat-transfer coefficient for a smooth tube of diameter d_o is $\varepsilon_{\Delta T}(d_r/d_o)^{3/4}$. For instance, when evaluating the advantage of re-tubing a smooth-tube condenser with finned tubes having diameter over fins equal to the OD of the smooth tubes, one would calculate as for smooth tubes but using a vapour-side, heat-transfer coefficient equal to the smooth tube (with diameter d_o) value multiplied by $\varepsilon_{\Delta T}(d_r/d_o)^{3/4}$ with $\varepsilon_{\Delta T}$ given by equation (47).

3. For tubes where 'fin efficiency effects' become significant, an iterative scheme has been developed (Briggs and Rose [16]).

Acknowledgement—The author is grateful to Dr Adrian Briggs for helpful discussions and computational assistance.

REFERENCES

1. W. Nusselt, Die Oberflachenkondensation des Wasserdampfes, *Z. Ver. Dt. Ing.* **60,** 541–546, 569–575 (1916).
2. H. Masuda and J. W. Rose, An experimental study of condensation of refrigerant-113 on low integral fin tubes, *Proc. Int. Symp. Heat Transfer, Beijing*, Vol. 2, paper no. 32 (1985); also in *Heat Transfer Science and Technology*, pp. 480–487. Hemisphere, Washington, D.C. (1987).
3. H. Masuda and J. W. Rose, Condensation of ethylene glycol on horizontal finned tubes, *Trans. ASME J. Heat Transfer* **110,** 1019–1022 (1988).
4. K. O. Beatty and D. L. Katz, Condensation of vapors on outside of finned tubes, *Chem. Engng Prog.* **44,** 55–70 (1948).
5. H. Honda, S. Nozu and K. Mitsumori, Augmentation of condensation on horizontal finned tubes by attaching a porous drainage plate, *Proc. ASME–JSME Thermal Engng Joint Conf.*, Vol. 3, pp. 289–296 (1983).
6. T. M. Rudy and R. L. Webb, An analytical model to predict condensate retention on horizontal, integral-fin tubes, *Proc. ASME–JSME Thermal Engng Joint Conf.*, Vol. 1, pp. 373–378 (1983).
7. T. M. Rudy and R. L. Webb, An analytical model to predict condensate retention on horizontal integral-fin tubes, *Trans. ASME J. Heat Transfer* **107,** 361–368 (1985).
8. H. Masuda and J. W. Rose, Static configuration of liquid fins on horizontal tubes with low radial fins, *Proc. R. Soc. Lond.* **A420,** 125–139 (1987).
9. R. Gregorig, Hautcondensation an feingewelten Oberflachen bei Beruksichtigung der Oberflachenspannungen, *Z. Angew. Math. Phys.* **5,** 36–49 (1954).
10. V. A. Karkhu and V. P. Borovkov, Film condensation of vapor at finely-finned horizontal tubes, *Heat Transfer–Sov. Res.* **3,** 183–191 (1971).
11. V. G. Rifert, A new method for calculating rates of condensation on finned tubes, *Heat Transfer—Sov. Res.* **12,** 142–147 (1980).
12. R. L. Webb, T. M. Rudy and M. A. Kedzierski, Prediction of the condensation coefficient on horizontal integral-fin tubes, *Trans. ASME J. Heat Transfer* **107,** 369–376 (1985).
13. T. Adamek and R. L. Webb, Prediction of film condensation on horizontal integral-fin tubes, *Int. J. Heat Mass Transfer* **33,** 1721–1735 (1990).
14. H. Honda and S. Nozu, A prediction method for heat transfer during film condensation on horizontal low integral-fin tubes, *Trans. ASME J. Heat Transfer* **109,** 218–225 (1987).
15. S. P. Sukhatme, B. S. Jagadish and P. Prabhakaran, Film condensation of R-11 vapour on single horizontal enhanced condenser tubes, *Trans. ASME J. Heat Transfer* **112,** 229–234 (1990).
16. A. Briggs and J. W. Rose, Effect of 'fin efficiency' on a model for condensation on a horizontal, integral-fin tube, *Int. J. Heat Mass Transfer* **37**(Suppl. 1), 457–463 (1994).
17. A. Briggs, X.-L. Wen and J. W. Rose, Accurate heat-transfer measurements for condensation on horizontal integral-fin tubes, *Trans. ASME J. Heat Transfer* **114,** 719–726 (1992).
18. X.-L. Wen, Filmwise condensation on horizontal integral-fin tubes, Ph.D. Thesis, Univ. London (1990).
19. A. S. Wanniarachchi, P. J. Marto and J. W. Rose, Film condensation of steam on horizontal finned tubes: effect of fin spacing, *Trans. ASME J. Heat Transfer* **108,** 960–966 (1985).
20. A. S. Wanniarachchi, P. J. Marto and J. W. Rose, Film condensation of steam on horizontal finned tubes: effect of fin spacing, thickness and height, *Multiphase Flow and Heat Transfer*, ASME-HTD Vol. 47, pp. 93–99 (1985).
21. P. J. Marto, D. Zebrowski, A. S. Wanniarachchi and J. W. Rose, An experimental study of R-113 film condensation on horizontal finned tubes, *Trans. ASME J. Heat Transfer* **112,** 758–767 (1990).
22. A. G. Michael, P. J. Marto, A. S. Wanniarachchi and J. W. Rose, Filmwise condensation of R-113 on horizontal integral-fin tubes of different diameters, *Proc. 9th Int. Heat Transfer Conf.*, Vol. 3, pp. 15–20 (1990).
23. T. C. Carnavos, An experimental study: condensing R-11 on augmented tubes, ASME Paper No. 80-HT-54, 19th National Heat Transfer Conference, Orlando, Florida (1980).
24. D. L. Katz, R. E. Hope, S. C. Datsko and D. B. Robinson, Condensation of Freon-12 with finned tubes, Part 1—Single horizontal tubes, *J. Am. Soc. Ref. Engng* **53,** 211–217 (1947).